optotune
shaping the future of optics

Application Note:
Field-of-View Expansion

Optotune AG | Bernstrasse 388 | CH-8953 Dietikon | Switzerland
Phone +41 58 856 3000 | www.optotune.com | info@optotune.com

optotune
shaping the future of optics

Table of Contents

Optotune AG | Bernstrasse 388 | CH-8953 Dietikon | Switzerland
Phone +41 58 856 3000 | www.optotune.com | info@optotune.com

optotune
shaping the future of optics

1 Introduction

Machine vision systems have fundamental limitations with respect to resolution, field-of-view, and depth of focus. Angular resolution and the field-of-view are conflicting specifications, limited by the size and resolution of the image sensor.

The field of view of an imaging system is given by the focal length f of the objective and the image sensor size S:

$$\mathrm{FOV} = 2\tan^{-1}\frac{S}{2f}$$

The depth of field of an imaging system with focal length f, focus or object distance d, the f-number N and the circle of confusion c:

$$\mathrm{DOF} \approx \frac{2d^2Nc}{f^2}$$

Extending the FOV while maintaining high resolution is crucial for a variety of applications. For example, in public surveillance of train stations or airports, a large scene needs to be imaged with the required resolution to do detailed object detection or face recognition. Another example is traffic sign detection in autonomous driving, which benefits from FOV expansion by enabling to read signs at a larger distance.

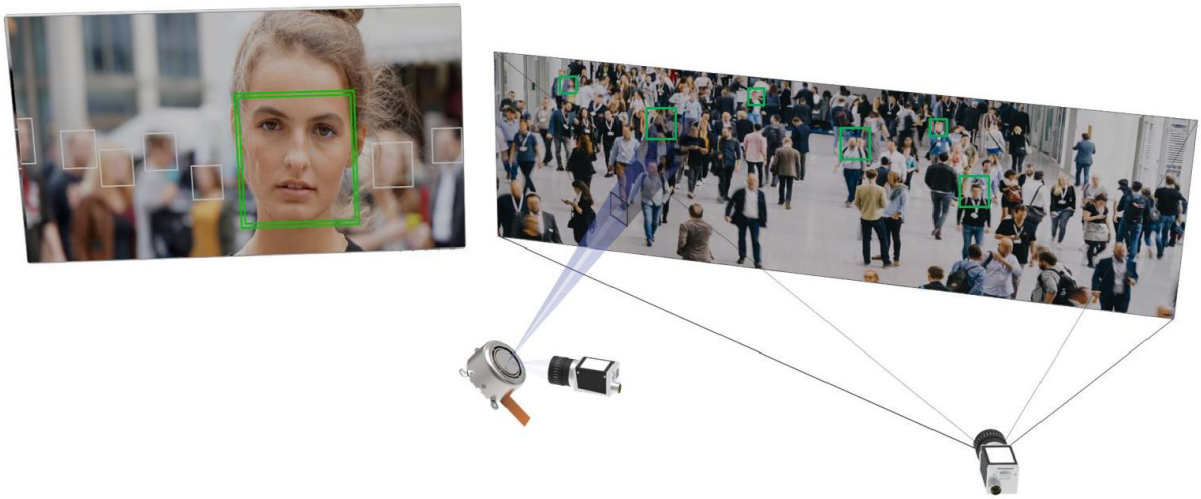

Figure 1: FOV expansion and area of interest selection using a 2D fast steering mirror.

Other applications where good resolution and a large FOV are beneficial are barcode scanning and iris recognition. To maintain high resolution, the barcode or the human eye need to be accurately positioned to be within the camera's FOV. This limits the ease-of-use of such imaging systems or may make it necessary to use multiple devices to cover the necessary FOV.

1.1 Mimicking the Human Eye

An elegant way to satisfy the extreme resolution and field-of-view requirements that these applications pose is to combine a 2D fast steering mirror with a liquid lens. The mirror is used to select a small area of interest within a large FOV while the liquid lens allows to quickly adapt the focus. This replicates the principle of a human eye.

Optotune AG | Bernstrasse 388 | CH-8953 Dietikon | Switzerland
Phone +41 58 856 3000 | www.optotune.com | info@optotune.com

To bring a lot of light to the camera it is beneficial to have a large mirror size. 2D-MEMS mirrors have very limited angular travel range and are generally too small. On the other hand, simply combining two single axis scan mirrors (galvo mirrors) in series is also not ideal, because the second mirror needs to be considerably bigger than the first, leading to bulky systems.

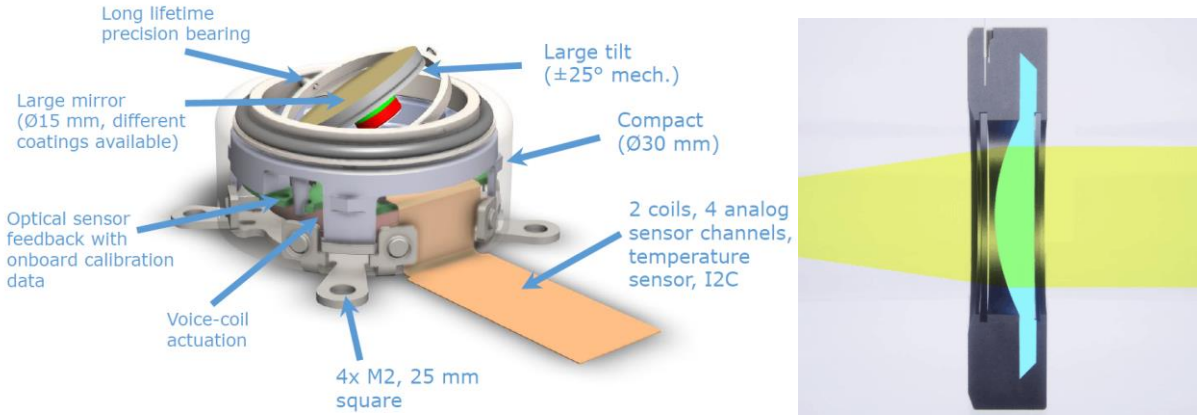

Figure 2: Main technological benefits of Optotune's MR-15-30 fast steering mirror and working principle of the focus tunable lens (EL-16-40).

Optotune's 2D fast steering mirror MR-15-30 with its 15 mm aperture and large ±25° scan range as well as the EL-16-40 with its unrivalled 16 mm clear aperture are both ideally suited for this application, allowing for a compact and flexible solution.

1.2 Development Kit

Optotune offers a Development Kit for FOV expansion. This application note describes how it works.

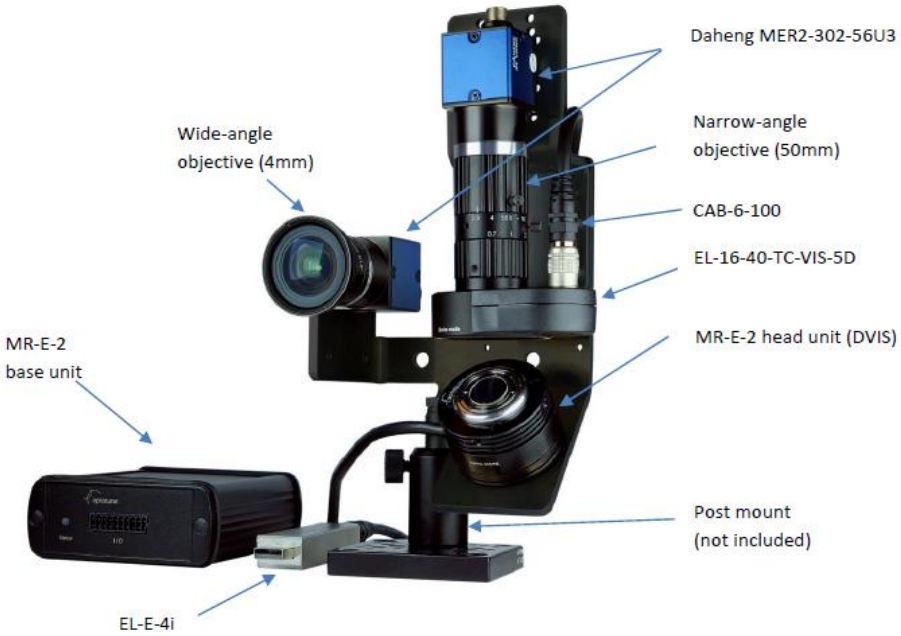

Optotune AG | Bernstrasse 388 | CH-8953 Dietikon | Switzerland
Phone +41 58 856 3000 | www.optotune.com | info@optotune.com

2 Camera Calibration

The simplest and most widely used camera model is the that of a pinhole camera. Figure 3 shows how points in the target or focal plane (x_t, y_t) get mapped onto the image plane (x_c, y_c) of the camera. For simplicity, the image plane is thought to be in front of the pinhole, at a distance equal to the focal length.

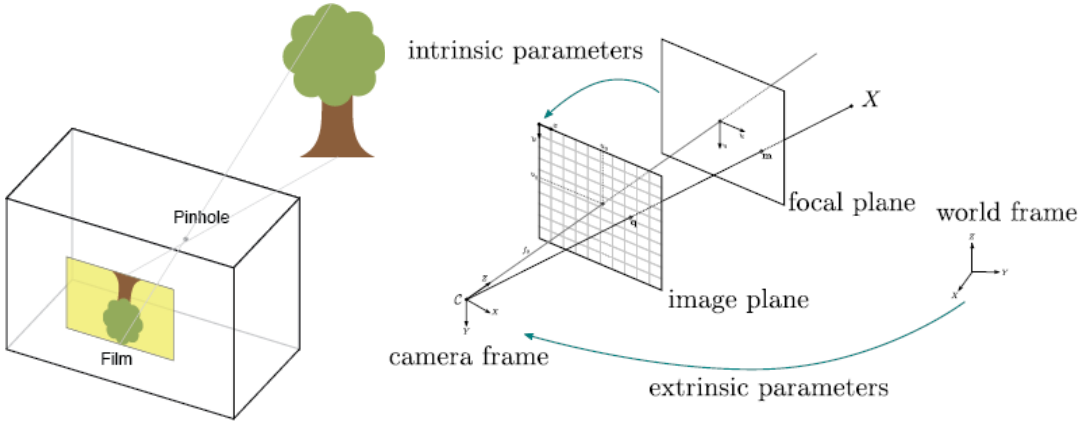

Figure 3: Pinhole camera model on the left and associated intrinsic and extrinsic calibrations on the right.

This simple model can be represented by the following relation written in homogenous coordinates

$$\begin{bmatrix} x_c \\ y_c \\ 1 \end{bmatrix} = \boldsymbol{K} \begin{bmatrix} \boldsymbol{R} & \boldsymbol{t} \end{bmatrix} \begin{bmatrix} x \\ y \\ z \\ 1 \end{bmatrix}$$

$$\text{where } \boldsymbol{K} = \begin{bmatrix} f_x & 0 & c_x \\ 0 & f_y & c_y \\ 0 & 0 & 1 \end{bmatrix}, \boldsymbol{R} = \boldsymbol{R}^{-\mathsf{T}} \text{ and } \boldsymbol{t} \in \mathbb{R}^3.$$

The extrinsic parameters, i.e. the rotation matrix $\boldsymbol{R}$ and the translation vector $\boldsymbol{t}$, describe the location and orientation of the world frame with respect to the camera frame. We can simplify the above equation by selecting normalized coordinates (x_t, y_t) on a target plane perpendicular to the optical axis at unit distance:

$$\begin{bmatrix} x_c \\ y_c \\ 1 \end{bmatrix} = \boldsymbol{K} \begin{bmatrix} x_t \\ y_t \\ 1 \end{bmatrix}.$$

This parametrization with only two coordinates makes sense because a camera on its own cannot determine how far an actual object is away from the image plane. Without knowing actual object dimensions, just the angles to the object are known.[1]

While for an ideal pinhole camera $f_x = f_y = f$ it makes sense to allow for a small difference in this parameter that can come from an imperfect sensor or from lens misalignment. The factors c_x and c_y are usually close to half of the image width and height, but can differ due to lens decentering.

For wide angle imaging systems, this linear camera model does not provide enough fidelity. Therefore, additional nonlinear terms need to be added to account for lens distortion. A common model is

$$x_{c,\text{distorted}} = x_c(1 + k_1 r^2 + k_2 r^4 + k_3 r^6) + 2p_1 x_c y_c + p_2(r^2 + 2{x_c}^2)$$
$$y_{c,\text{distorted}} = y_c(1 + k_1 r^2 + k_2 r^4 + k_3 r^6) + p_1(r^2 + 2{y_c}^2) + 2p_2 x_c y_c$$

[1] Using a liquid lens for focusing, however, yields a depth measurement without any domain knowledge. See https://www.optotune.com/s/Distance-measurement-using-an-Optotune-focus-tunable-lens.pdf.

Optotune AG | Bernstrasse 388 | CH-8953 Dietikon | Switzerland
Phone +41 58 856 3000 | www.optotune.com | info@optotune.com

with $r = \sqrt{{x_c}^2 + {y_c}^2}$ and k_1, k_2, k_3 describing radial distortion, namely pincushion and barrel distortion, and p_1, p_2 describing tangential distortion.

A standard and practical technique to fit these parameters to a set of measurements was found by Zhang[2]. All that is required is a set of pictures of a flat checkerboard taken from a variety of positions and angles. An example implementation can be found here[3]. Typically, at least about 10 views of the checkerboard are required for a precise model fit.

Optotune Cockpit allows to import a calibration matrix and distortion vector as defined above for the face recognition demo program. Make sure to check that $c_x < c_y$ due to the portrait format of the wide-angle camera.

Figure 4: One of the images of a checkerboard used to calibrate camera.

[2] Zhang, Zhengyou. (2000). A Flexible New Technique for Camera Calibration. Pattern Analysis and Machine Intelligence, IEEE Transactions on. 22. 1330 - 1334. 10.1109/34.888718.
[3] https://docs.opencv.org/3.4/dc/dbb/tutorial_py_calibration.html

Optotune AG | Bernstrasse 388 | CH-8953 Dietikon | Switzerland
Phone +41 58 856 3000 | www.optotune.com | info@optotune.com

3 Mirror Coordinate System

3.1 Definition of the XY Coordinate System

We define a coordinate system to calibrate the internal optical feedback mechanism and relate it with physical mirror position. This coordinate system is a cartesian coordinate system with axes X and Y. The X-axis is perpendicular to the cable protruding from the mirror head and the Y-axis is parallel to this cable. The numerical values on the axes are unitless and defined via the maximum deflection of the mirror in optical angles, i.e. 50°. Along each axis, a deflection of +50° corresponds to a value of +1 and a deflection of -50° corresponds to a value of -1. This corresponds to the projection observed on a screen if the mirror reflects a laser beam travelling along the z-axis, incident on its center. For example, the analytical relationship between deflection angle θ and coordinate system value x along the x-Axis is:

$$\frac{\tan(\theta)}{\tan(50°)} = x$$

The figure below illustrates the relationship between deflection on-axis and coordinate system value using three examples.

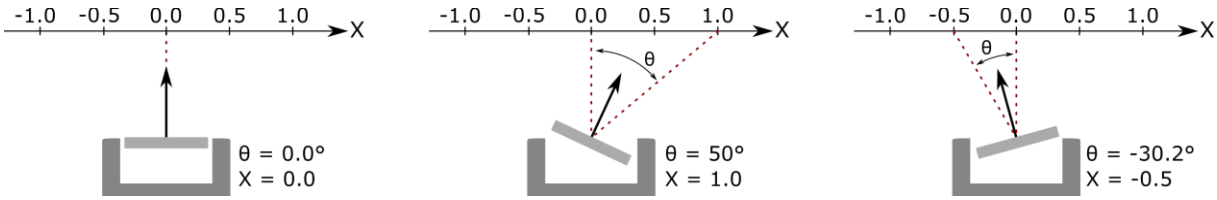

The mirror has a maximum deflection of 25° in every direction. Therefore, in the XY coordinate system a unit circle with radius 1 contains all accessible values, as shown in gray color in the figure below.

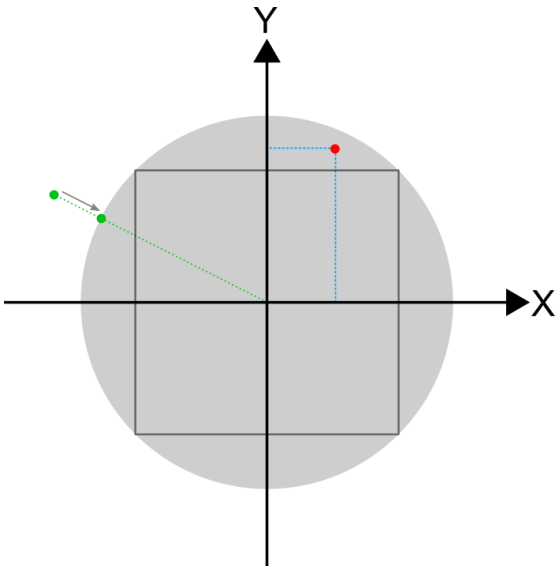

The mirror can access every possible combination of X and Y values for both X and Y < 0.7 (black square in the figure above). If one of the XY values exceeds 0.7, the other value must decrease, so that at any time $X^2 + Y^2 \leq 1$ (the red dot in the figure above is an example). The firmware automatically reduces XY positions outside the accessible unit circle by moving them to the nearest edge of the unit circle (green dots in the figure above). This behavior prevents mirror and driver damage.

Optotune AG | Bernstrasse 388 | CH-8953 Dietikon | Switzerland
Phone +41 58 856 3000 | www.optotune.com | info@optotune.com

When driving the mirror in open loop mode, it is possible to reach angles larger than 25°, which correspond to XY values bigger than 1. However, these angles are outside the guaranteed and calibrated range of the mirror and calibration accuracy can vary significantly.

3.2 Transformation Between Different Cartesian Projection Coordinates

When using the mirror in a scanning system, typically the arrangement with 0° AOI is not practical, since incident and reflected beam paths would overlap. The figure below shows the general case: The mirror with its middle point M and normal vector $\boldsymbol{n}_m$ rotates around the center of rotation C and reflects an incoming beam, specified by a point P_0 and a unit vector $\boldsymbol{n}_0$. The reflected beam starts at point P_1 and has the direction of the unit vector $\boldsymbol{n}_1$. Finally, the reflected beam hits a target plane at the point P_2, where the target plane is located at a distance D from the undeflected mirror center and a has the normal vector $\boldsymbol{n}_t$.

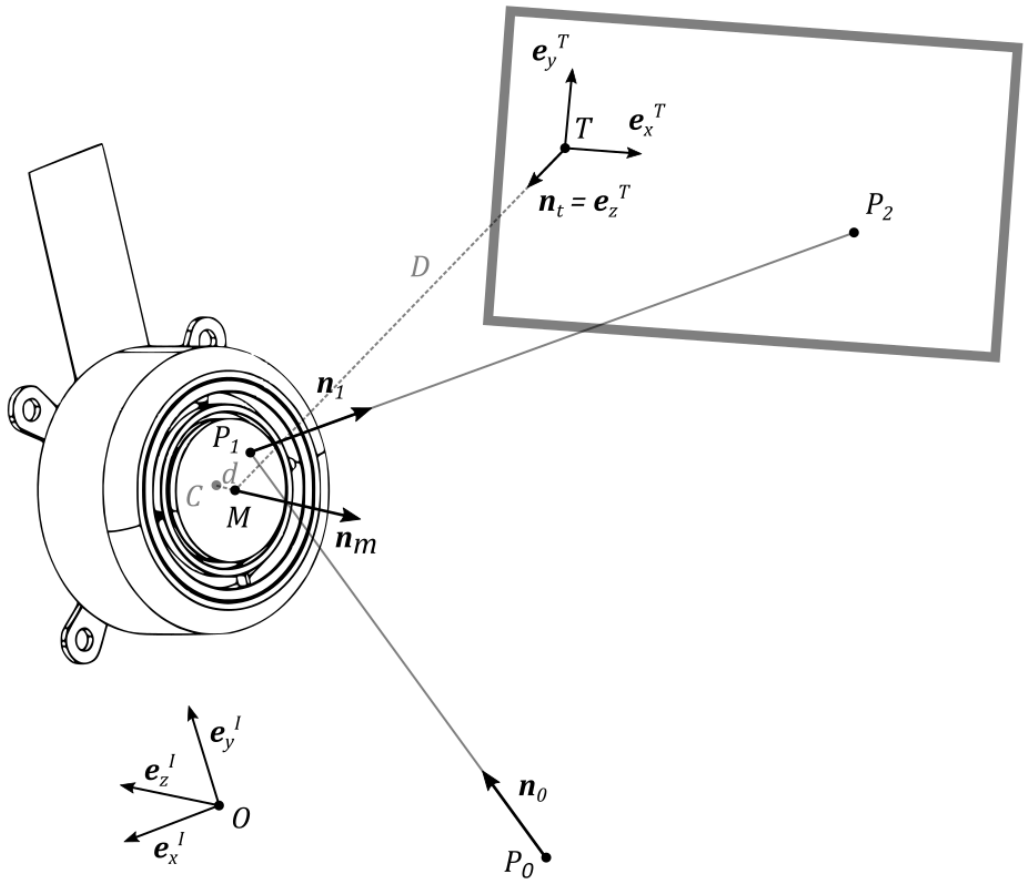

This general arrangement captures distortion effects due to

- AOI of the incoming beam
- Rotated target plane
- Off-centered incoming beam
- Distant center of rotation

The vector analysis to calculate the beam path is straightforward. First, inserting the equation for the incoming beam $\boldsymbol{r} = \boldsymbol{r}_{OP_0} + t \cdot \boldsymbol{n}_0\,,\ t \in \mathbb{R}$ into the equation for the mirror plane $(\boldsymbol{r} - \boldsymbol{r}_{OM}) \cdot \boldsymbol{n}_m = 0$, yields the intersection point P_1

$$\boldsymbol{r}_{OP_1} = \boldsymbol{r}_{OP_0} + t_1 \cdot \boldsymbol{n}_0, \qquad \text{where} \quad t_1 = \frac{(\boldsymbol{r}_{OM} - \boldsymbol{r}_{OP_0}) \cdot \boldsymbol{n}_m}{\boldsymbol{n}_0 \cdot \boldsymbol{n}_m}.$$

Optotune AG | Bernstrasse 388 | CH-8953 Dietikon | Switzerland
Phone +41 58 856 3000 | www.optotune.com | info@optotune.com

Note that $\boldsymbol{r}_{OM} = \boldsymbol{r}_{OC} + d \cdot \boldsymbol{n}_m$.

Then, the reflected beam is obtained by applying the law of reflection

$$\boldsymbol{n}_1 = \boldsymbol{n}_0 - 2 \cdot (\boldsymbol{n}_0 \cdot \boldsymbol{n}_m) \cdot \boldsymbol{n}_m.$$

Finally, we calculate the intersection point with the target plane P_2

$$\boldsymbol{r}_{OP_2} = \boldsymbol{r}_{OP_1} + t_2 \cdot \boldsymbol{n}_1, \qquad \text{where} \quad t_2 = \frac{(\boldsymbol{r}_{OT} - \boldsymbol{r}_{OP_1}) \cdot \boldsymbol{n}_t}{\boldsymbol{n}_1 \cdot \boldsymbol{n}_t}.$$

We can now express the vector $\boldsymbol{r}_{TP_2} = \boldsymbol{r}_{OP_2} - \boldsymbol{r}_{OT}$ in target plane coordinates

$${}_T\boldsymbol{r}_{TP_2} = \boldsymbol{A}_{TI}\ {}_I\boldsymbol{r}_{TP_2} = \begin{bmatrix} x_t \\ y_t \\ 0 \end{bmatrix},$$

where $\boldsymbol{A}_{TI} = \boldsymbol{A}_{IT}{}^{-1} = \boldsymbol{A}_{IT}{}^{\top}$ is the orthogonal transformation matrix between the frames of reference I and T.

In a simplified case, for an incoming beam hitting the mirror centered and d assumed to be zero, we have $P_1 = M = C$ and one can explicitly calculate the mirror orientation from projected coordinates.

$$\boldsymbol{n}_m = \frac{\boldsymbol{n}_1 - \boldsymbol{n}_0}{\|\boldsymbol{n}_1 - \boldsymbol{n}_0\|}, \qquad \text{where } \boldsymbol{n}_1 = \frac{\boldsymbol{r}_{MP_2}}{\|\boldsymbol{r}_{MP_2}\|} \text{ and } \boldsymbol{r}_{MP_2} = \boldsymbol{r}_{MT} + \boldsymbol{r}_{TP_2}.$$

Note that this simplification still captures the distortion introduced by the AOI of the incoming beam, which is by far the most important one to consider.

For convenience, in the following, the origin O is placed at the undeflected mirror center: $O = P_1 = M = C$.

The above equations can be used to transform between normalized mirror coordinates $(x,\ y)$ and target plane coordinates $(x_t,\ y_t)$:

$(x,\ y) \rightarrow \boldsymbol{n}_m \rightarrow (x_t,\ y_t)$:

1. By definition of the mirror coordinates set ${}_I\boldsymbol{n}_0 = \begin{bmatrix} 0 \\ 0 \\ 1 \end{bmatrix}$ and ${}_I\boldsymbol{r}_{MP_2} = \begin{bmatrix} x\ D\tan 50° \\ y\ D\tan 50° \\ -D \end{bmatrix}$. So, ${}_I\boldsymbol{n}_1$ is obtained by normalizing $\begin{bmatrix} x \\ y \\ -1/\tan 50° \end{bmatrix}$ and the mirror normal by calculating $\boldsymbol{n}_m = \frac{\boldsymbol{n}_1 - \boldsymbol{n}_0}{\|\boldsymbol{n}_1 - \boldsymbol{n}_0\|}$.
2. Redefine the actual incoming beam $\boldsymbol{n}_0$ and target plane ($\boldsymbol{A}_{TI}$ and D). Using the known mirror normal $\boldsymbol{n}_m$, calculate ${}_T\boldsymbol{r}_{TP_2}$ using the above equations and extract (x_t, y_t), i.e. the first two components of ${}_T\boldsymbol{r}_{TP_2}$.

$(x_t,\ y_t) \rightarrow \boldsymbol{n}_m \rightarrow (x,\ y)$:

1. Specify the actual incoming beam $\boldsymbol{n}_0$ and target plane ($\boldsymbol{A}_{TI}$ and D).
   Calculate ${}_I\boldsymbol{r}_{MP_2} = \boldsymbol{A}_{TI}{}^{\top} \begin{bmatrix} x_t \\ y_t \\ -D \end{bmatrix}$ and normalize to get ${}_I\boldsymbol{n}_1$, then obtain the mirror normal from $\boldsymbol{n}_m = \frac{\boldsymbol{n}_1 - \boldsymbol{n}_0}{\|\boldsymbol{n}_1 - \boldsymbol{n}_0\|}$.

Optotune AG | Bernstrasse 388 | CH-8953 Dietikon | Switzerland
Phone +41 58 856 3000 | www.optotune.com | info@optotune.com

2. By definition of the mirror coordinates redefine ${}_I\boldsymbol{n}_0 = \begin{bmatrix}0\\0\\1\end{bmatrix}$ and $\boldsymbol{A}_{TI} = \mathbf{1}$. Using the mirror normal $\boldsymbol{n}_m$ from the previous step, calculate ${}_I\boldsymbol{n}_1 = {}_I\boldsymbol{n}_0 - 2 \cdot \left({}_I\boldsymbol{n}_0 \cdot {}_I\boldsymbol{n}_m \right) \cdot {}_I\boldsymbol{n}_m$. Scale this vector with a constant factor to get the vector $\begin{bmatrix} x \\ y \\ -1/\tan 50° \end{bmatrix}$, from which x and y can be extracted.

As an example, consider the following example arrangement:

The incoming beam in the yz-plane hits the mirror centered at a 45° incidence angle. The target plane is placed perpendicular to the reflected beam for an undeflected mirror, i.e. when $x = y = 0$.

$$ {}_I\boldsymbol{n}_0 = \frac{1}{\sqrt{2}}\begin{bmatrix}0\\-1\\1\end{bmatrix},\ {}_I\boldsymbol{r}_{OP_0} = \begin{bmatrix}0\\1\\-1\end{bmatrix},\ \boldsymbol{A}_{TI} = \begin{bmatrix}1 & 0 & 0\\ 0 & \cos 45° & -\sin 45° \\ 0 & \sin 45° & \cos 45°\end{bmatrix},\ D = 1700\ \text{mm},\ d = 1.3\ \text{mm} $$

The below plots show the distortions introduced in this case. For reference, also the 100° FOV is shown, which the mirror would achieve for 0° AOI.

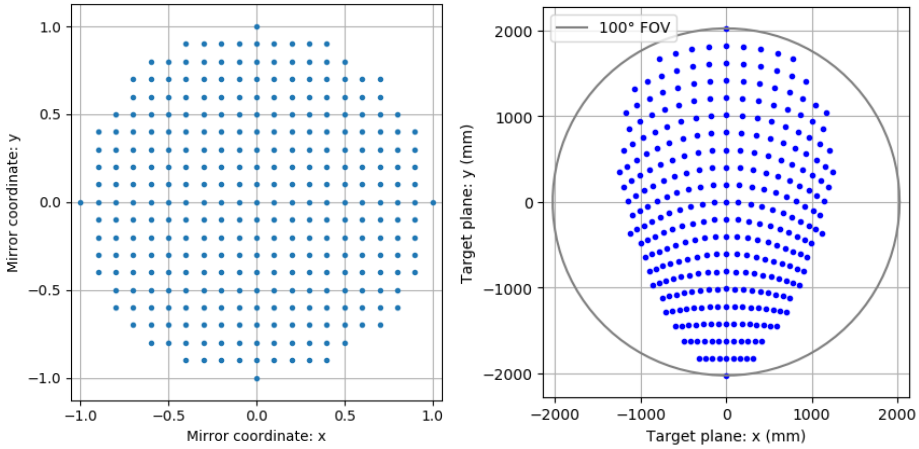

Optotune AG | Bernstrasse 388 | CH-8953 Dietikon | Switzerland
Phone +41 58 856 3000 | www.optotune.com | info@optotune.com

4 Image rotation

When the mirror is in the undeflected position as shown in Figure 5, the camera sees a vertically flipped, i.e. mirrored image. This is simple to correct and sometimes there is even a separate camera setting for flipping the image. However, when the mirror is scanned, objects in the resulting image still appear rotated in general. The angle of rotation depends on the normal vector $\boldsymbol{n}$ of the mirror. The configuration below is identical to the configuration in the Optotune FOV Expansion Development Kit, with the camera mounted vertically and the mirror mounted at 45°.

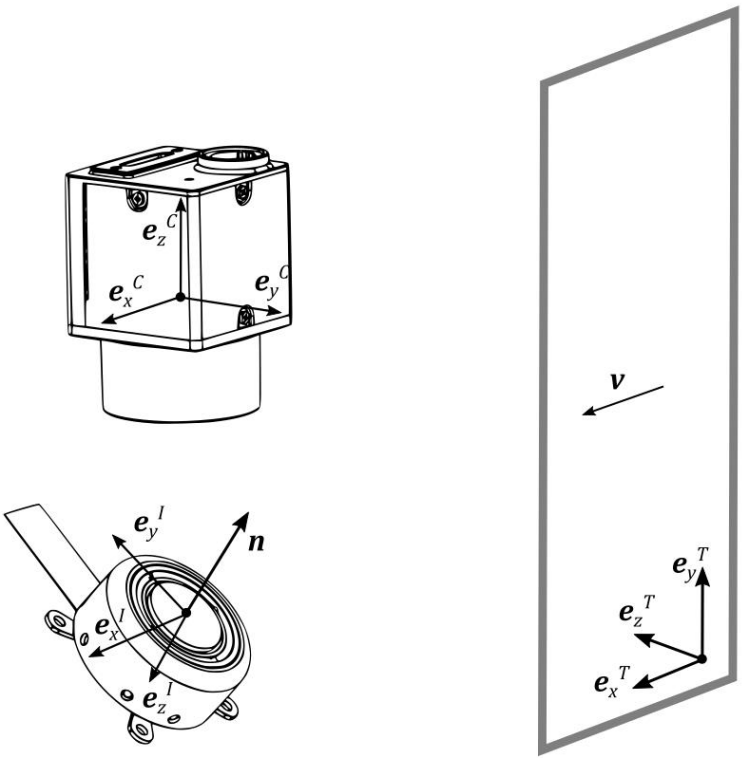

Figure 5: Three different frames of reference, aligned with the object or target plane, the mirror housing and the camera respectively.

Looking at how a certain vector $\boldsymbol{v}$ gets mapped onto the camera will allow calculating this angle. For simplicity consider $\boldsymbol{v}$ aligned with the horizontal direction of the target frame T, which in turn is aligned with the mirror's x-direction, i.e. $\boldsymbol{v} = \boldsymbol{e}_x{}^T = \boldsymbol{e}_x{}^I$. When $\boldsymbol{v}$ is mirrored, it gets mapped to the vector $\boldsymbol{r}$ through the householder transformation

$$\boldsymbol{r} = (\mathbf{1} - 2\boldsymbol{n}\boldsymbol{n}^\top)\,\boldsymbol{v} = (\mathbf{1} - 2\boldsymbol{n}\boldsymbol{n}^\top)\,\boldsymbol{e}_x{}^I\,.$$

Expressing this equation in the frame I yields

$${}_I\boldsymbol{r} = \begin{bmatrix} 1-2n_x{}^2 & * & * \\ -2n_xn_y & * & * \\ -2n_xn_z & * & * \end{bmatrix}\begin{bmatrix}1\\0\\0\end{bmatrix} = \begin{bmatrix} 1-2n_x{}^2 \\ -2n_xn_y \\ -2n_xn_z \end{bmatrix},$$

Where ${}_I\boldsymbol{n} = [n_x \quad n_y \quad n_z]^\top$ and all entries that do not contribute to the matrix-vector product are marked with *.

By projecting this vector $\boldsymbol{r}$ onto the image sensor plane the rotation angle can be calculated as follows

$$\varphi = \tan^{-1}\frac{r_y}{r_x}$$

$$r_x = {}_I\boldsymbol{r}\cdot {}_I\boldsymbol{e}_x{}^C = {}_I\boldsymbol{r}\cdot \boldsymbol{A}_{IC}\,{}_C\boldsymbol{e}_x{}^C$$

Optotune AG | Bernstrasse 388 | CH-8953 Dietikon | Switzerland
Phone +41 58 856 3000 | www.optotune.com | info@optotune.com

$$r_y = {}_I\boldsymbol{r} \cdot {}_I\boldsymbol{e}_y{}^C = {}_I\boldsymbol{r} \cdot \boldsymbol{A}_{IC}\, {}_C\boldsymbol{e}_y{}^C ,$$

where $\boldsymbol{A}_{IC}$ is found as a rotation around x by 135°

$$\boldsymbol{A}_{IC} = \begin{bmatrix} 1 & 0 & 0 \\ 0 & \cos 135° & \sin 135° \\ 0 & -\sin 135° & \cos 135° \end{bmatrix}.$$

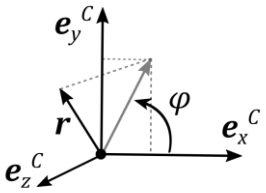

Figure 6: Projection of $\boldsymbol{r}$ onto the image sensor plane. After being mirrored, the horizontal vector $\boldsymbol{v}$ appears rotated by φ.

With all of the above the rotation for the setup as shown in Figure 5 the angle $\varphi \in (-\pi/2\,,\, \pi/2)$ becomes

$$\varphi = -\tan^{-1} \frac{\sqrt{2}\, n_x\, (n_y + n_z)}{1 - 2{n_x}^2} \ .$$

Note that in order to rotate the image back, it is necessary to rotate the camera image by the angle $-\varphi$.

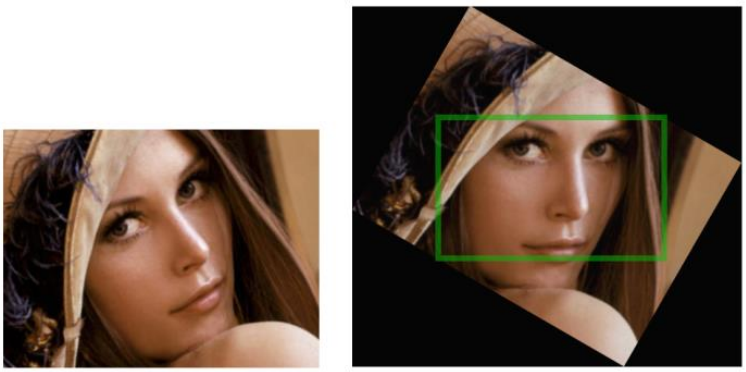

Figure 7: Rotated image as captured by the camera (A) and the back-rotated image with cropped image having largest area (B).

When using the straightened image, it is necessary to either pad the corner areas or to crop the image. The cropping can for example be done as shown in Figure 7 (B) by maximizing the area. Another choice would be to maximize area while keeping the aspect ratio constant. It is obvious that for large rotation angles a significant portion of the image gets discarded that way. However, for computer vision algorithms such as face recognition or barcode scanning, rotating the image back is typically not necessary.

Optotune AG | Bernstrasse 388 | CH-8953 Dietikon | Switzerland
Phone +41 58 856 3000 | www.optotune.com | info@optotune.com

5 Face detection

Figure 8 shows the program flow of the face detection demo program in Optotune Cockpit. The demo algorithm detects a face in the wide-angle overview image, and provides a focused high-resolution image of that face using the tunable lens and the 2D mirror:

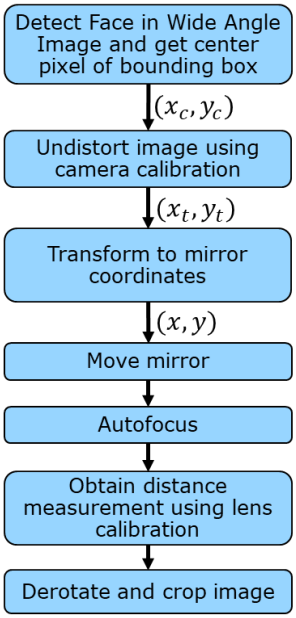

Figure 8: Flowchart of face detection demo program in Optotune Cockpit.

- For face detection we use a neural net by Linzai https://github.com/Linzaer/Ultra-Light-Fast-Generic-Face-Detector-1MB which was ported to C# by Takuya Takeuchi https://github.com/takuya-takeuchi/UltraFaceDotNet
- Autofocus with distance measurements are described in here: www.optotune.com/s/Distance-measurement-using-an-Optotune-focus-tunable-lens.pdf
- The following parameters can be adjusted in the autofocus algorithm to find a good compromise between accuracy and speed:
  lens settling time (ms), lower focal power limit (dpt), upper focal power limit (dpt), coarse step (dpt), fine step (dpt).
- In Optotune Cockpit, two calibrations are available for the distance from focus measurement using the 50mm and 75 mm objectives respectively. The calibration is valid only when the manual focus is set to infinity. A custom calibration can be done by measuring the focal power FP needed to focus to different working distances and fit the parameters a, b, c to the data using the simple model:

$$\text{Working distance} = \frac{a}{FP + b} + c$$

Optotune AG | Bernstrasse 388 | CH-8953 Dietikon | Switzerland
Phone +41 58 856 3000 | www.optotune.com | info@optotune.com

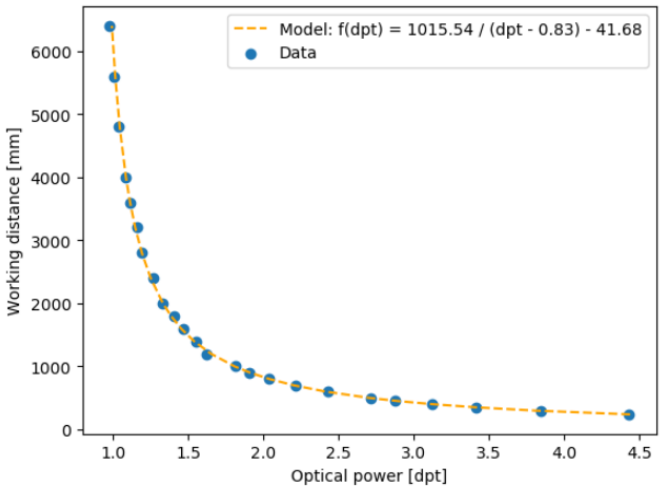

- The complete list of parameters can be imported into Optotune Cockpit as a json formatted text file. After closing Optotune Cockpit, the software stores an updated json file to the users Appdata folder (path=%appdata%), which will be automatically loaded at the next startup.

Optotune AG | Bernstrasse 388 | CH-8953 Dietikon | Switzerland
Phone +41 58 856 3000 | www.optotune.com | info@optotune.com

6 Image Stitching

This chapter describes how to stitch a panoramic gigapixel image using the FOV expansion development kit.

Figure 9: Example of stitched image with gigapixel resolution.

Another example image can be found on our website.

6.1 Choice of positions for the mirror

Due to the projection distortion described in chapter Transformation Between Different Cartesian Projection Coordinates3.2, a uniform spacing in terms of mirror coordinates will not result in a uniform spacing in the scene. Instead, one needs to calculate the mirror coordinates that lead to a uniform spacing in the target plane. The sampling density should be chosen to yield a certain overlap between neighboring images, typically about 20%-40%. More overlap increases the number of pictures to be captured and also increases computational effort to stitch the image. A too small overlap, on the other hand, makes the feature matching process more difficult.

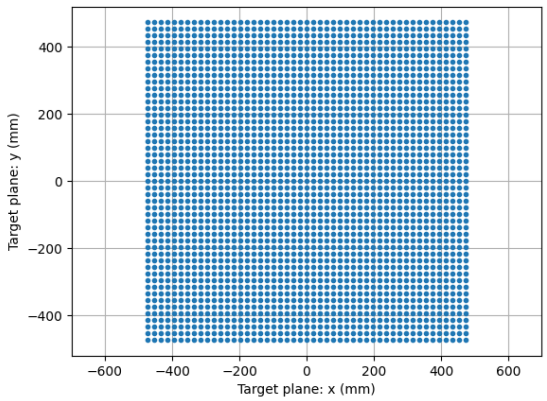

After concerting to mirror coordinates, only the points within the range of actuation of the mirror a circle of radius 1 are selected, as all other points are outside of the mirror's travel limit.

Optotune AG | Bernstrasse 388 | CH-8953 Dietikon | Switzerland
Phone +41 58 856 3000 | www.optotune.com | info@optotune.com

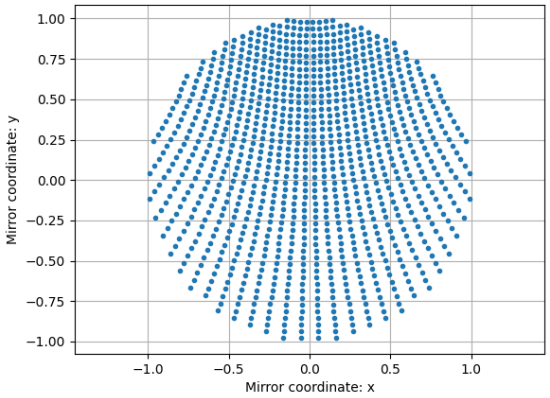

Below the back-projection of those points in XY coordinates can be seen.

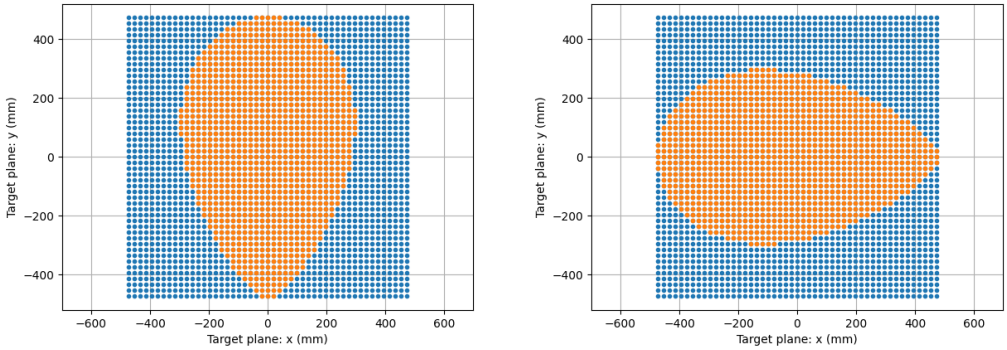

Due to the shape of the zone of capture and the fact that a landscape picture is usually preferred, the setup can be rotated in order to get a bigger horizontal range than a vertical one.

6.2 Example Python Script for Image Acquisition

We provide a sample Python script to acquire images using the FOV Expansion Development Kit, using the outlined coordinate transformations. The output of the script is:

- Set of images uniformly acquired across FOV, numbered row by row
- Hugin.csv: Stored coordinates for each image (image position and image rotation) to be imported in the next step to facilitate the stitching process.

6.3 Stitching process

We describe the stitching process based on the free, yet powerful Hugin software.

Optotune AG | Bernstrasse 388 | CH-8953 Dietikon | Switzerland
Phone +41 58 856 3000 | www.optotune.com | info@optotune.com

1) Import all images

2) (Optional) Get an initial picture distribution and image rotation according to mirror positions. This step allows to limit picture comparisons to neighboring images. From the command line use the command "pto_var --set-from-file filename --output=output.pto project.pto" with the file (filename="Hugin.csv") created with the python script taking the pictures. This should place all pictures in proximity to the final position after stitching. If the process results in a good result you can jump to point 7).

3) Create control points (CP): For the feature matching create a new CP detector (cpfind.exe with argument "—linearmatch -o %o %s") which will detect matches between adjacent images (in the order of the import). This method will require an additional step to align the rows in the panorama, but the complexity of the CP detector will drastically decrease. The alternative CP detector *multirow* has higher computational complexity.

4) Create control points (connecting rows): Connect different rows by adding CP manually. It is advised to create CP for the pictures in the edges. No need to create CP along all the row as the *prealigned* method will do this work. Another method is to manually move rows in the preview window to align them correctly and run the CP detector with *prealigned* method 7).

5) Anchor the center image: Select the image and use the context menu to define the reference image.

6) Optimization step: This process will optimize the position of the pictures to minimize the mismatches In the control points. There is no need to optimize translation in the Geometric parameters since the setup as long as the setup is stationary. Do not forget to previously anchor a picture close to the center.

7) Autodetect control points of prealigned images (considering only overlapping images): Create a new CP detector with argument "--prealigned -o %o %s". This process will create CP between overlapping pictures which do not have CP in common. This step is to align images within rows, or also globally, if step 2) was successful.

8) (Optional) Create horizontal/vertical lines: This helps to avoid distortion in the stitched image. Add lines, e.g. edges of buildings, in different parts of the image for a better result, adding a lot of lines in same area of the FOV is not useful.

9) Verification + erasing bad CP: The bad CP can easily be identified in the CP table; usually they are the ones with large distances (sort accordingly). Verify those and delete the ones that are not correct (due to repetitive patterns in the pictures such as on building, a lot of bad CPs can appear). Be sure to redo the optimization step from time to time as you delete false control points.

10) Photometric optimization: Select multiple photometric parameters to optimize notably the vignetting[4] parameters. Do not forget to set as anchor for exposure a picture that is not over/under exposed. (Right click on Photos panel).

11) Stitching process: In *Stitcher* tab, calculate the FOV and optimal size before stitching. If you don't want to see the edges of the panorama and instead a rectangle, use the crop button. It is strongly advised to use *Multiblend* a significantly faster drop-in alternative to *Enblend* for the blending process (https://horman.net/multiblend/). "Due to Enblend's O(n^2) complexity, compared to Multiblend's O(n) linear time complexity, this speed advantage increases to 300x for a gigapixel mosaic". The use of "--wideblend" argument is advised.

[4] Vignetting could be improved by having an entrance pupil of the objective tailored to the size of the mirror. Optotune may consider developing a custom lens for FOV expansion in the future.

Optotune AG | Bernstrasse 388 | CH-8953 Dietikon | Switzerland
Phone +41 58 856 3000 | www.optotune.com | info@optotune.com

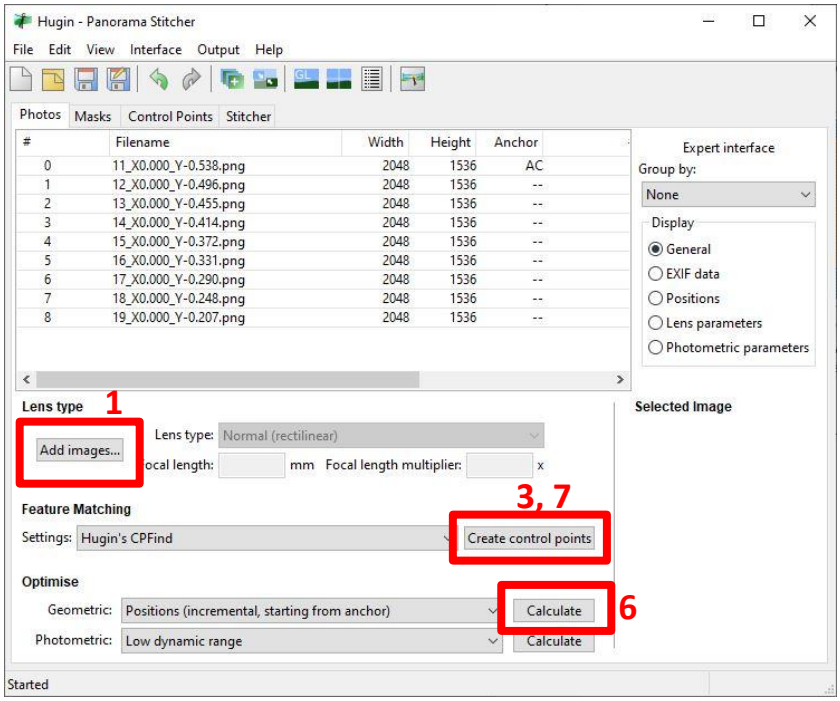

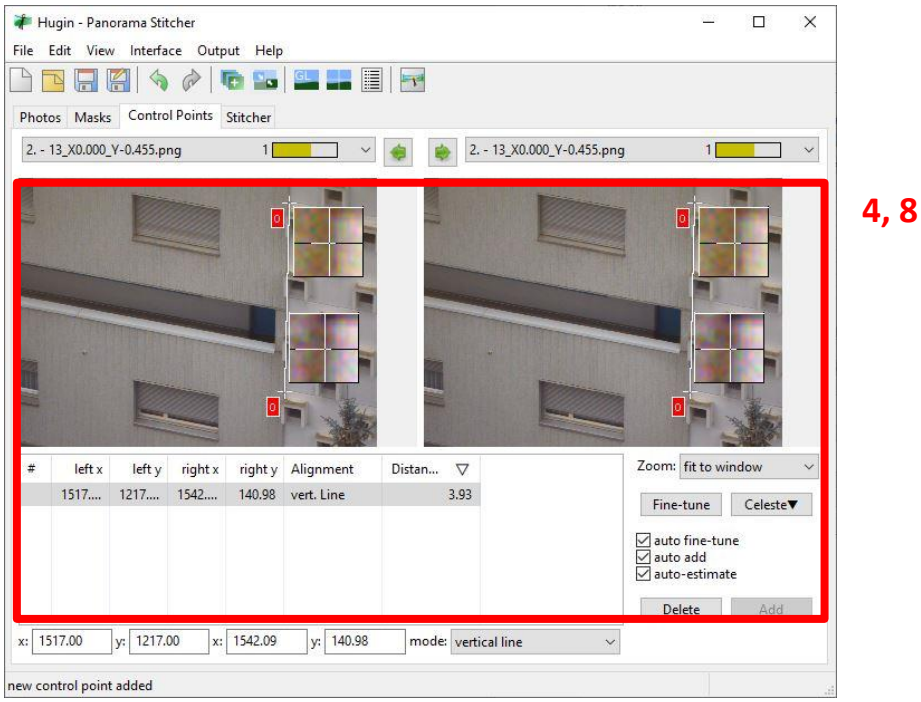

Optotune AG | Bernstrasse 388 | CH-8953 Dietikon | Switzerland
Phone +41 58 856 3000 | www.optotune.com | info@optotune.com

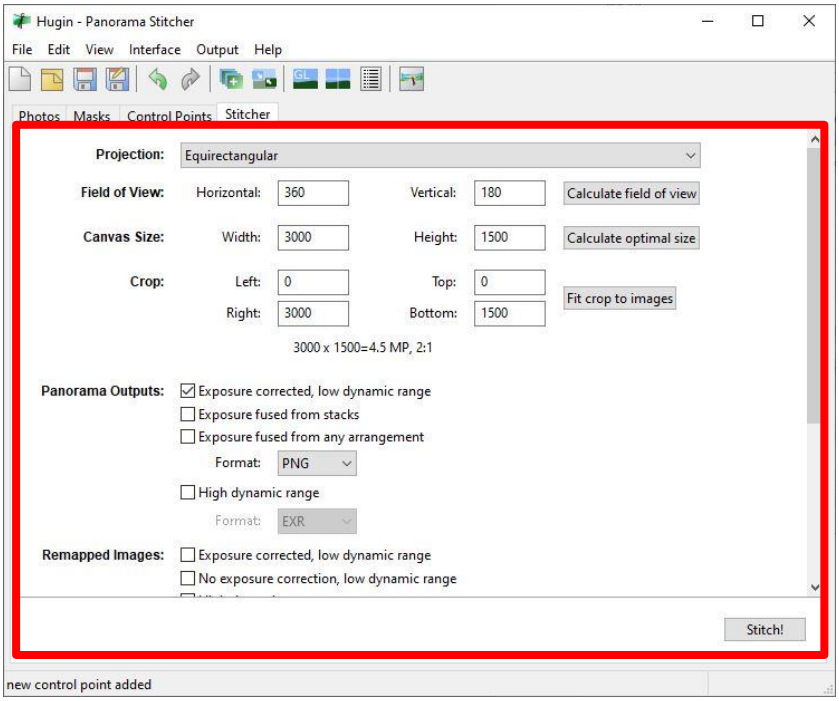

10

Optotune AG | Bernstrasse 388 | CH-8953 Dietikon | Switzerland
Phone +41 58 856 3000 | www.optotune.com | info@optotune.com